HHS Public Access

Author manuscript

ACS Biomater Sci Eng. Author manuscript; available in PMC 2021 January 13.

Published in final edited form as:

ACS Biomater Sci Eng. 2020 January 13; 6(1): 277–287. doi:10.1021/acsbiomaterials.9b01482.

Ferritin Nanocage Conjugated Hybrid Hydrogel for Tissue Engineering and Drug Delivery Applications

Roya Samanipour[†,‡,∇], **Ting Wang**[†,§,∇], **Moritz Werb**[†,∇], **Hamed Hassannezhad**[†], **Juan Manuel Ledesma Rangel**[†], **Mina Hoorfar**[‡], **Anwarul Hasan**[⊥,#], **Chang Kee Lee**[*,‖], **Su Ryon Shin**[*,†]

[†]Division of Engineering in Medicine, Department of Medicine, Brigham and Women's Hospital, Harvard Medical School, Cambridge, Massachusetts 02139, United States

[‡]Department of Mechanical Engineering, School of Engineering, University of British Columbia, Kelowna V6T 1Z4, Canada

[§]School of Medicine, Jiangsu University, Zhenjiang, Jiangsu 212013, China

[‖]Korea Packaging Center, Korea Institute of Industrial Technology, Bucheon 31056, Republic of Korea

[⊥]Department of Mechanical and Industrial Engineering, College of Engineering, Qatar University, 2713 Doha, Qatar

[#]Biomedical Research Centre (BRC), Qatar University, 2713 Doha, Qatar

Abstract

Hydrogels have recently been attractive in various drug delivery and tissue engineering applications because of their structural similarities to the natural extracellular matrix. Despite enormous advances in the application of hydrogels, poor mechanical properties and lack of control for the release of drugs and biomolecules act as major barriers for widespread clinical applications. To overcome these challenges, we developed both physically and covalently conjugated nanocage-laden hydrogels between the surface of the nanocage and a gelatin methacryloyl (GelMA) hydrogel matrix. Ferritin and its empty-core equivalent apoferritin were used as nanocages that could be easily incorporated into a GelMA hydrogel via physical bonding. To fabricate covalently conjugated nanocage-laden GelMA hydrogels, ferritin and apoferritin were chemically modified to present the methacryloyl groups, ferritin methacryloyl (FerMA) and apoferritin methacryloyl (ApoMA), respectively. The covalently conjugated FerMA- and ApoMA-

[*]**Corresponding Authors:** sshin4@bwh.harvard.edu. Phone: (617) 835-1164. Fax: (617) 768-8477 (S.R.S.).; withs@kitech.re.kr. Phone: +82 (032) 624 4774. Fax: +82 (032) 624 4770 (C.K.L.).

[∇]Author Contributions

R.S., T.W., and M.W. contributed equally to this work.

ASSOCIATED CONTENT

Supporting Information

The Supporting Information is available free of charge on the ACS Publications website at DOI: 10.1021/acsbiomaterials.9b01482. F-actin/DAPI staining of NIH-3T3 fibroblasts encapsulated in 5 wt % GelMA hydrogels with 10 s UV exposure time after 7 days of culture (Figure S1); phase contrast images of NIH-3T3 fibroblasts encapsulated in 5 wt % GelMA hydrogels with 10 s UV exposure time after 2 days of culture (Figure S2) (PDF)

The authors declare no competing financial interest.

GelMA hydrogels offered a better ability to tune mechanical properties compared with those prepared by direct dispersion of ferritin and apoferritin into GelMA hydrogels with physical bonding, without affecting their porosity or cell growth. Furthermore, the ability of the nanocage to release small chemical compounds was confirmed by performing a cumulative release test on fluorescein isothiocyanate (FITC) encapsulated apoferritin and ApoMA incorporated GelMA hydrogels by pH stimulus. Thus, the nanocage incorporated hydrogels have emerged as excellent materials for drug delivery and tissue engineering applications.

Graphical Abstract

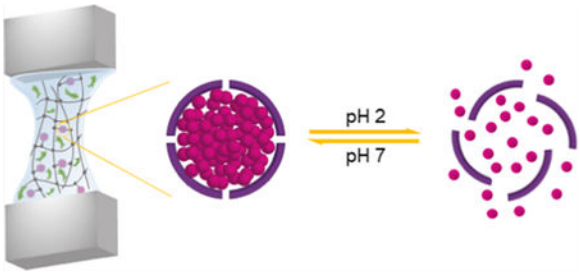

Keywords

hydrogel; nanocage; ferritin; apoferritin; drug delivery; tissue engineering

INTRODUCTION

Engineered hydrogels have recently drawn a lot of attention for applications in the field of biomedicine such as tissue regeneration, organ-on-a-chip, and drug delivery due to their high biocompatibility and the similarity of physical properties to the native extracellular matrix (ECM).[1–4] In terms of tissue engineering application, the mechanical properties of hydrogels play important roles in regulating cell-to-cell interactions and cell-to-ECM interactions and in directing the differentiation and maturation of cells. However, the low mechanical strength and fragile nature of the hydrogels still hinder the feasibility of hydrogels' clinical applications.[5–7] Furthermore, hydrogels themselves, which are mainly composed of single or multiple biopolymers, rarely possess the superior biological properties of native ECMs and the pharmacological properties to improve therapeutic functions.[8,9] To increase the utilization of hydrogels in clinical and pharmacological fields, nanoparticle incorporated composite or hybrid hydrogels have been developed to adjust the biological and physical properties of hydrogels to resemble native tissues and bring controlled release of biological compounds (e.g., drug and genes) to adapt to the criteria required for their specific applications.[1,10–14] Recent reports indicate that most nanoparticles have been able to solve one issue. For example, liposome-based nanoparticles are well-defined in achieving drug or gene delivery functions; however, the incorporation of liposomes makes it difficult to improve or tune the mechanical properties of the hydrogel due to their weak mechanical properties.[15,16] Also, metal-based or polymer-based nanoparticles have been widely used to improve the mechanical properties of hydrogels. However, biological compounds, which are mostly immobilized on the surface, or embedded polymeric networks of nanoparticles, could

be damaged or degraded via direct exposure to biological environments (containing various enzymes to degrade biological compounds) and during chemical modification processes that require harsh materials such as organic solvents or high/low temperatures or pH conditions. Therefore, only a few nanoparticles have achieved all advantages at the same time, such as tunable mechanical and physicochemical properties and delivery potential with controlled release of small molecules/drugs under specific conditions along with less cytotoxicity.[17]

To address the above challenges, nanocages that can encapsulate various biological compounds are an excellent candidate due to their unique features. A major advantage of nanocages is that they can protect against the degradation and denaturation of encapsulated substances under biological environments. Also, the nanocages can be chemically modified by cross-linkers or various receptors to immobilize specific matrices and achieve targeted delivery platforms without damaging the encapsulated substances. Among various nanocages, naturally derived ferritin, which is a spherical cage consisting of 24 protein subunits, was selected.[18,19] With a pH-dependent assembly property, ferritin can store various substances (i.e., drugs, various types of metals, RNA, DNA, etc.) and release them in specific conditions (e.g., changes in pH and specific receptors), which could achieve a targeted drug delivery system.[20–23] In terms of improving mechanical properties, ferritin can be physically bound on the polymeric networks through the carboxylic acid and amino groups on its protein shell.[24,25] The peptide shell interacts as a spring, passing the force to the stable core and therefore tuning the mechanical properties of the hydrogels.[24] Furthermore, ferritin is highly resistant to chemical and physical denaturants, including heating to high temperatures (>80 °C). Therefore, owing to its uniform nanosize (around 12 nm diameter), excellent stability, core–shell structure, unique surface properties, and easy chemical modification, ferritin has emerged as a capable protein-based nanocage to achieve our aim of controlling the release of drugs and improving the mechanical properties of hydrogels.

To create ferritin reinforced hybrid hydrogels, a gelatin methacryloyl (GelMA), a photo-cross-linkable hydrogel, was used due to its excellent biocompatibility and biological properties with cell-binding sites.[8,9] Here, we report a simple approach to chemically modify the surfaces of ferritin and apoferritin with methacrylate (MA) groups to facilitate covalently bonding them on GelMA networks while keeping their release properties under specific conditions. Mechanical properties of the hydrogels incorporated with ferritin via covalent bonding were improved compared with those made with physical bonding. Also, the reinforced hybrid hydrogels showed less cellular toxicity and good cellular growth with a high concentration of ferritin. A drug release strategy was evaluated as a proof of concept using fluorescein isothiocyanate (FITC)-laden apoferritin/GelMA hybrid hydrogels for drug delivery applications. Consequently, ferritin incorporated hybrid hydrogels with enhanced mechanical properties and drug delivery potential could play important roles in improving the cell behaviors and are expected to be a promising biomaterial for various biomedical applications.

MATERIAL AND METHODS

Materials.

Gelatin (Type A, 300 bloom from porcine skin), methacrylate anhydride (MA), NaOH pellets, NaCl, 3-(trimethoxysilyl)-propyl methacrylate (TMSPMA), and ferritin and apoferritin (both from equine spleen) were purchased from Sigma-Aldrich (St. Louis, Missouri). Irgacure 2959 (2-hydroxy-1-(4-(hydroxyethoxy)-phenyl)-2-methyl-1-propanone), as a photoinitiator (PI), was acquired from Ciba Specialty Chemicals Incorporated (Basel, Switzerland). Dulbecco's phosphate-buffered saline (DPBS), Dulbecco's modified Eagle's medium (DMEM), fetal bovine serum (FBS), and penicillin–streptomycin were bought from Invitrogen (Waltham, Massachusetts). Dialysis membrane tubes, Slide-A-Lyzer Dialysis cassette, glass slides, and coverslips were purchased from Thermo Fisher Scientific (Waltham, Massachusetts). Alexa Fluor 488 Phalloidin, 4′,6-diamidino-2-phenylindole (DAPI), LIVE/DEAD kit, and fluoraldehyde o-phthaldialdehyde (OPA) were acquired from Thermo Fisher Scientific (Waltham, Massachusetts). Omnicure S2000 (EXFO Photonic Solutions Incorporation, Quebec City, Canada) was used for photo-cross-linking. The device for mechanical testing was the 5942 Single Column Tabletop Model testing system from Instron, an ITW company (Illinois Tool Works Incorporation, Glenview, Illinois).

Synthesis of GelMA.

GelMA was synthesized following a protocol based on a previous work.[9] In short, 10 wt % gelatin was dissolved into DPBS at 50 °C (using a magnetic stirrer). Then, 8 mL of MA was added dropwise to reach a final concentration of 8 wt % MA. After a 2 h reaction at 50 °C, the solution was diluted 1:1 with DPBS (previously warmed) and dialyzed against distilled (DI) water with a dialysis membrane (MW CO 12 000–14 000, Fisher Scientific) for 5 days at 40 °C, maintaining a constant stirring and changing the DI water every 12 h. The dialyzed GelMA prepolymer solution was stored at −80 °C and, according to experimental needs, freeze-dried for 5 days to prepare for use.

Fabrication of Ferritin and Apoferritin Methacrylation (FerMA/ApoMA).

First, 1 mL of ferritin solution (52 mg/mL) was diluted by the same amount of DPBS in a stirring glass vial in cold room conditions (4 °C). Then, 20 μL of MA was added slowly, and the solution was stirred overnight at the same speed for at least 12 h. The FerMA was dialyzed with a dialysis cassette (Slide- A-Lyzer, MW CO 12 000–14 000, Fisher Scientific) against normal saline solution (9 g of sodium-chloride dissolved in 1 L of distilled water) for 3 days. Apoferritin was delivered at a lower concentration (13 mg/mL) than ferritin (52 mg/mL). Therefore, the apoferritin solution did not need further dilution. The procedure for creating ApoMA is the same as for creating FerMA. To a 1 mL apoferritin solution, 20 μL of methacrylate anhydride was added dropwise. The reaction and dialysis were done the same way.

Characterization of Methacrylation.

To qualify the methacrylation of primary amine groups on the protein surfaces of ferritin and apoferritin, a commonly known fluoraldehyde assay was used. OPA reacts with free amine

groups ($-NH_2$) giving a blue fluorescent product. The excitation and emission maximums are at 340 and 455 nm. The fluorescent signal can be measured, correlating directly with the number of free amine groups in the solution. Solutions with the same concentration of proteins (100 μg/mL) need to be prepared. The same amount of fluoraldehyde OPA reagent solution was added, and in a quick manner the fluorescent spectrum was measured. The differences compared to a reference (DPBS, in which the proteins are diluted) were recorded, and the degree of substitution was calculated with the following equation:

$$Z = \left(1 - \frac{I_{\text{protein-methacrylate}} - I_{\text{reference}}}{I_{\text{protein}} - I_{\text{reference}}}\right) \times 100$$

where Z is the degree of substitution and $I_{\text{protein–methacrylate}}$, I_{protein}, and $I_{\text{reference}}$ are the intensities of the fluorescent signal for the methacrylated protein, the unreacted protein, and the reference, respectively.

Transmission Electron Microscope (TEM) Analysis.

Diluted nanocage-laden solutions were applied onto holeycarbon-film-coated grids and then stained with 1% uranyl acetate solution. The negatively stained samples were observed by Talos L120C TEM (Thermofisher).

Hydrogel Fabrication.

The ferritin-GelMA, FerMA-GelMA, apoferritin-GelMA, and ApoMA-GelMA were obtained by dissolving 5 wt % freeze-dried GelMA and 0.5% (w/v) of the PI in PBS for 1 h at 80 °C. Different concentrations of ferritin, FerMA, apoferritin, and ApoMA were added to the solution and mixed. Then, 30 μL of the prepolymer solution was pipetted on an even surface with a spacer height of 600 μm. The drop was covered with a TMSPMA-coated glass slide, producing a cylindrical specimen with 600 μm height and 6 mm diameter. Then, it was exposed to UV light with an intensity of 6.9 mW/cm^2 and a distance of 8 cm for cross-linking.

Characterization of Mechanical Properties.

The mechanical properties of the hydrogel materials were tested using a mechanical testing system, Instron 5942 Single Column Tabletop Model, an ITW company (Illinois Tool Works Incorporation, Glenview, Illinois), equipped with a computer-based analysis/control system (Bluehill version 3) while the hydrogel disks were compressed at 1 mm/min until they cracked. The compressive modulus was evaluated for 0–15% strain of the stress–strain curve, which is the slope of the corresponding linear region. Ultimate stress was defined as right before the hydrogel fractured. For a tensile test, the samples were prepared in the dimensions of 20 mm length, 10 mm width, and 1 mm height. The ends of the samples were fixed in between 2 cm poly(methyl methacrylate) (PMMA) slides by applying a superglue. Failure strain and tensile strength were defined using strain at the point of failure and the maximum stress, respectively. The stress–strain curves were plotted up to the point of fracture of the sample. The area under the stress–strain curve was calculated as toughness

Scanning Electron Microscopy (SEM) Imaging.

For analyzing the morphological features of hydrogels, hydrogels were frozen and dried. Then, the samples were piloted with a LEICA LEO S430i scanning electron microscope.

Cell Studies.

NIH-3T3 fibroblasts were suspended in a prepolymer solution (2×10^6 cells/mL) and cross-linked via photo-cross-linking to fabricate hydrogels. The cell-laden hydrogels were cultured in DMEM supplemented with 10% FBS and 100 units/mL penicillin-streptomycin (all purchased from Invitrogen) at 37 °C and 5% CO_2. Viability was characterized by a LIVE/DEAD Viability/Cytotoxicity kit. Samples were incubated with calcein (green) and ethidium homodimer-1 (red) at dilutions of 0.5:1000 and 2:1000, respectively, for 10 min at 37 °C. A fluorescent microscope (Zeiss, Axio Observer.D1, Germany) was used to obtain fluorescence images. Image J software was used to analyze fluorescence images. F-actin/DAPI staining was performed on day 7 of culture; samples were fixed with 4% paraformaldehyde for 30 min and then permeabilized with 0.1% Triton X-100 for 30 min at room temperature. The samples were stained by Alexa Fluor 488 phalloidin with a 1:40 dilution ratio for 45 min and then were counterstained with DAPI with a dilution ratio of 1:1000 for 15 min.

Fabrication of FITC-laden Apoferritin Hydrogel and Characterization.

First, 1 mg/mL apoferritin and ApoMA were prepared in the HCl solution with pH 2. Then, 2 mg/mL FITC solution was prepared (FITC powder was dissolved in DPBS) and added in a prepared apoferritin/ApoMA solution. The solution was kept overnight at 4 °C for disassembling the ApoMA and apoferritin. Afterward, 20 μL of 1 M NaOH was added to the solution to neutralize it. Then, the solution was dialyzed with a dialysis cassette (Slide- A-Lyzer, MWCO 12000, Fisher Scientific) for 2 days at 4 °C. Finally, 5 wt % GelMA and 0.5% photoinitiator were mixed with 2 mg/mL FITC-loaded apoferritin/ApoMA and cross-linked as explained in the fabrication of the hydrogel part. Each FITC-laden apoferritin-GelMA and FITC-laden ApoMA-GelMA hydrogel specimen (600 μm height and 6 mm diameter) was placed in 500 μL of PBS, and accumulative release tests were performed at different time points (0, 6, 12, 24, 48, and 72 h).

Calculation of Cumulative Release.

For calculating the cumulative FITC release test, first a calibration curve graph was plotted. Different concentrations of FITC solution (mg/mL) were prepared, and the intensity of each solution was measured. Then, the calibration curves were plotted (intensity vs concentration of FITC) in which each concentration of FITC was corresponded to the intensity. Second, the FITC release test was performed. The FITC-laden GelMA-apoferritin hydrogel discs were put in well plates, and a volume of buffer (pH 2) was added to each well plate. At the first time point, the buffer was taken out and the intensity was measured, and a new volume of buffer was added to the well plate. The drug concentration corresponding to this intensity was calculated using the calibration curve. Then, the concentration (mg/mL) was multiplied by the volume (mL) of the buffer to get the mass of the released FITC (mg). In the next time point, the release amount would be the current release amount plus the previous release

amount. This continued until the point where we did not see any intensity, which meant that all of the FITC was released. For plotting the percentage of cumulative release for the graph, the amount of released FITC was added to the total drug concentration that we had in the beginning.

Statistical Analysis.

One-way analysis of variance (GraphPad Prism 5.02) statistical data was used for analyzing the data when appropriate. The data represents the mean and standard deviation. Quantified data were categorized as significantly different when $p < 0.05$ using Tukey's multiple comparison test.

RESULTS AND DISCUSSION

Methacrylate groups were conjugated into ferritin and apoferritin by reaction with methacrylate anhydride (Figure 1a,1b) to achieve covalent bonding on the GelMA matrix. To determine the conversion of amines, a fluoraldehyde assay was used. The fluorescent signals give direct information of free amine groups and therefore are an indicator of the percentage of the reacted amine groups. The results showed that the degrees of methacrylation of FerMA and ApoMA were ~85% and ~92%, respectively (Figure 1c), confirming that a reasonable number of amine groups on ferritin and apoferritin had conjugated with methacrylate groups. Furthermore, the core–shell structural integrity of the ferritin and apoferritin after the methacrylation process was verified using a high-resolution TEM (HRTEM) (Figure 1d). Comparing the HRTEM images of ferritin with FerMA and apoferritin with ApoMA, it could be concluded that both protein shells of apoferritin and ferritin did not disassemble and were undamaged during the methacrylation reaction, retaining their nanocage structure with a uniform size (~10 nm), which would be necessary for controlled release potential and improvement of mechanical properties.

Hybrid GelMA hydrogels incorporated with varying concentrations of ferritin ("ferritin-GelMA hydrogel"), FerMA ("FerMA-GelMA hydrogel"), apoferritin ("apoferritin-GelMA hydrogel"), and ApoMA ("ApoMA-GelMA hydrogel") were fabricated using the photo-cross-linking method (Figure 2a). The visual change in the color of ferritin-GelMA and apoferritin-GelMA prepolymer solutions when the concentration of nanocages increased is shown in Figure 2b. Here, as the ferritin concentration was increased, the prepolymer solution showed a stronger brownish yellow color because of ferritin's iron core. On the other hand, changes in the concentration of apoferritin, which does not have an iron core, in the prepolymer solution did not affect its visible properties and the solution remained colorless and transparent (Figure 2b). To initiate gelation of the prepolymer solution through cross-linking of methacrylate groups, Irgacure 2959 photoinitiator (PI), which is activated upon UV exposure in the range of 200–300 nm to create radical species, was used.[26] The absorbance of prepolymer solutions was investigated for different concentrations of ferritin and apoferritin (Figure 2c). By increasing the concentration of ferritin, the absorbance was significantly increased in the activation range of PI due to the increased number of iron cores. However, high and low concentrations of apoferritin (lack of iron cores) showed similar UV absorbance behavior, which could be attributed to the scattering from the protein

shell instead of absorbance by the core.[27] Therefore, we expect the ferritin-GelMA prepolymer solution to require longer UV exposure times to completely cross-link the hydrogels compared with those of the apoferritin-GelMA and pristine GelMA prepolymers.

One of the important challenges in hydrogel fabrication for tissue engineering applications is finding materials with high mechanical properties while maintaining a porous structure, which can contain a large amount of biological media and provide an area for cell growth and spreading. In previous studies, GelMA hydrogels have been well-known biomaterials that have a highly porous morphology, a high swelling ratio, and provide suitable matrices for cell growth and spreading.[9,28] A scanning electron microscope was used to compare the porosity and morphology of pristine GelMA and ferritin/FerMA incorporated hybrid GelMA hydrogels. Although the pore structure of the hydrogels might have changed during the freeze-drying process and conditions, it could be possible to compare the relative morphological changes among samples using SEM images and freeze-dried samples that were all prepared under the same conditions. As shown in Figure 2d, the porous structure of GelMA hydrogels was still maintained after the incorporation of ferritin and FerMA via both physical and covalent bonding. In addition, the smooth surface of the pore walls of the incorporated hydrogel confirmed that both ferritin and FerMA were homogeneously dispersed in GelMA prepolymer solutions without severe aggregation.

One of the major limitations of using hydrogels is their poor mechanical properties and fragile nature, resulting in inducing fast degradation and easily damaged shapes or structures. Instead of increasing the concentration of the polymer that could decrease the porous structures of the hydrogels and result in the inhibition of cellular behaviors, a naturally derived ferritin nanocage was used to improve and tune the mechanical properties. Besides the basic mechanical properties of the hydrogel and the incorporated nanoparticles, there are three important parameters that determine the mechanical properties of the nanocomposites: the nanoparticle architecture and nanoparticle–hydrogel and nanoparticle–nanoparticle interactions.[29] With regard to ferritin, nanocage–hydrogel interactions play a crucial role in the degree of mechanical reinforcement in nanocomposites.[24,25,30] To evaluate the effects of physically and covalently conjugated nanocages on the GelMA polymeric matrix, mechanical properties were analyzed on the various concentrations of ferritin, apoferritin, FerMA, and ApoMA incorporated GelMA hydrogels. Considering the UV absorbance of ferritin, apoferritin, FerMA, and ApoMA as shown in Figure 2c, the UV exposure time was an important factor affecting the mechanical properties of hybrid hydrogels. So, the effect of UV cross-linking time on the compressive moduli of 5 wt % GelMA hydrogels with various concentrations of ferritin and FerMA was investigated (Figure 3a–c). As a general trend in GelMA hydrogels with different ferritin concentrations, the compressive modulus positively correlated with the UV exposure time, reaching a plateau, followed by a slight downward trend after about 60 s of exposure. This was to be expected, as the hydrogels become fully cross-linked after sufficient exposure to UV irradiation, and therefore further exposure could not enhance the mechanical properties any further. Compressive moduli for 5 wt % GelMA hydrogels started at 2.36 kPa for 10 s UV exposure and reached a maximum at 6.24 kPa for 60 s UV exposure. Adding 0.1 mg/mL ferritin to GelMA significantly enhanced the compressive moduli of the hybrid hydrogels, giving the hydrogels compressive moduli ~3 times higher than that of a pristine GelMA

hydrogel. It was proposed that the functional groups (carboxylic acid (−COOH) and amino ($-NH_2$) groups) on the protein shell of ferritin could be combined with GelMA (hydroxyl (−OH) group) by forming hydrogen bonds.[25] Therefore, the protein shell could act as an elastic nanospring between the GelMA polymeric networks and the ferritin core to improve the mechanical properties of ferritin-GelMA hydrogels. However, when a further increase of ferritin concentration to 1.0 and 10 mg/mL was applied, the compressive modulus of the hydrogel was 10.8 kPa for 100 s and 8.9 kPa for 350 s, respectively, significantly lower compared with that of the 0.1 mg/mL ferritin-GelMA hydrogel. Even for higher ferritin concentrations (10 mg/mL) in the GelMA hydrogel, longer UV exposure times of more than 180 s were required to create the hydrogel form. There are several possibilities for this behavior. First, the absorbance at specific wavelengths for the activation of PI increased significantly with higher concentrations of ferritin. This high absorbance significantly decreased the transmittance of prepolymer solutions, resulting in a decreased cross-linking density of the ferritin-GelMA hydrogel. Second, ferritin is considered an antioxidant material in the body, which absorbs free radicals like radical scavengers that might induce the decrease of cross-linking networks of GelMA hydrogels during the photo-cross-linking process.[31] This behavior was observed in our previous studies high concentrations of carbon nanotubes (CNTs) act as radical scavengers, which decrease the cross-linking density, resulting in a decrease of stiffness in GelMA hydrogels.[11,32]

In contrast, 0.1 mg/mL FerMA-GelMA hybrid hydrogels, which have covalent networks, showed improved compressive moduli around ~4 times higher (17 kPa for 60 s) than those of both pristine GelMA hydrogels and ferritin-GelMA hydrogels. By increasing the concentration of FerMA to 1.0 mg/mL, the compressive modulus at 10 s UV exposure time decreased, which may be attributed to a higher absorption of UV light (Figure 3c). Due to the short period of UV exposure (10 s), higher concentrations of FerMA could not offset the effect of UV absorption, which attenuated the chain polymerization of the methacryloyl substitutions between FerMA and GelMA and between GelMA polymers. However, under longer UV exposure times of more than 20 s, the compressive modulus increased with increasing FerMA concentrations, which is a completely different behavior compared with physically conjugated ferritin-GelMA hydrogel systems (Figure 3a). The opposite effects of ferritin and FerMA concentrations on the mechanical properties of the GelMA hydrogels could be attributed to the two different interactions between physically bound ferritin and covalently bound FerMA on the GelMA polymer matrices. Incorporated FerMA does not compete for hydroxyl (−OH) groups on GelMA; therefore, more FerMA could additionally generate covalent networks, which could improve mechanical stiffness without hindering the interconnected network formation during GelMA cross-linking despite the high UV absorption. Overall, both physically incorporated ferritin and covalently incorporated FerMA had improved mechanical properties compared with pristine GelMA hydrogels. However, covalently incorporated FerMA showed better tunability of mechanical properties by increasing the concentration of the nanocage compared with physically incorporated ferritin hydrogels.

A similar study was performed on 5 wt % GelMA hydrogels with different concentrations of apoferritin and ApoMA (Figure 3d–f). Here, for a 0.1 mg/mL apoferritin-GelMA hydrogel, the compressive modulus increased ~2-fold compared with a pristine GelMA hydrogel. By

further increasing the apoferritin concentration to 1.0 mg/mL, the compressive modulus dropped significantly due to the stronger scattering from the protein. In the case of adding 0.1 and 1.0 mg/mL ApoMA, the hydrogel's mechanical properties were improved 2-fold compared with a pristine GelMA hydrogel with no significant difference between the two concentrations because of the same reasons the 1.0 mg/mL FerMA-GelMA hydrogel had higher UV absorption. The compressive modulus of the apoferritin-GelMA hydrogel was also lower compared with the improvement produced in the hydrogels by adding 0.1 mg/mL ferritin to GelMA (Figure 3a), which could be the result of the missing iron core in apoferritin.[24]

The tensile tests for ferritin- and FerMA-GelMA hydrogels with varying concentrations of nanocages are shown in Figure 3g. Both the ferritin and FerMA conjugated hydrogels showed linear stress–strain curves along with generally increased ultimate tensile strain and stress compared with pristine GelMA hydrogels. By increasing the concentrations of ferritin and FerMA, the ultimate tensile strain decreased. A similar trend was observed when different concentrations of apoferritin and ApoMA were added into GelMA hydrogels (Figure 3h). Similarly, the addition of apoferritin and ApoMA to GelMA hydrogels increased the ultimate tensile strain by approximately 20% for most of the hydrogels compared with pristine GelMA hydrogels except for the 1.0 mg/mL apoferritin-GelMA hydrogel, which reduced the ultimate tensile strain. In addition, we observed an improvement in the ultimate tensile stress of all hybrid hydrogels compared with pristine GelMA hydrogels. Therefore, all hybrid hydrogels were easily handled and stretched as shown in Figure 3i,j. Overall, the addition of the methacrylate forms of FerMA and ApoMA to GelMA hydrogels significantly improved both maximum elongation and ultimate tensile stress of the composite hydrogels (Figure 3k). However, in the case of physically incorporated ferritin and apoferritin, improvement in both ultimate strain and ultimate stress was observed only for the 0.1 mg/mL concentration, and a further increase in the concentration of apoferritin/ferritin to 1.0 mg/mL decreased the maximum elongation of the hydrogel to the level of a pristine GelMA hydrogel (Figure 3k).

To further specify the hydrogel, the toughness of different concentrations of GelMA incorporated with nanoparticles was evaluated. As shown in Figure 3l, the toughness for 5 wt % GelMA was 343.2 J/mm^3. Here, adding ferritin and its chemical derivatives significantly enhanced the toughness of the hydrogel in all cases. However, the toughest hybrid hydrogels were achieved by incorporating low concentrations of nanocages, where the toughness was enhanced by more than 135%. The corresponding values were 885.1, 809.8, 864, and 831.2 J/mm^3 for 0.1 mg/mL ferritin, 0.1 mg/mL FerMA, 0.1 mg/mL apoferritin, and 0.1 mg/mL ApoMA, respectively. For higher concentrations of nanocages, such as 1.0 mg/mL, the toughness decreased slightly in all cases compared with low concentrations. However, the lowest value of toughness obtained was 600.5 J/mm^3 for 1.0 mg/mL ferritin, which was still 75% higher than that of a pristine GelMA hydrogel. As described above, Shin et al. found that the properties of the PVA hydrogel such as mechanical strength, elastic modulus, and maximum elongation significantly increased compared with a pristine PVA hydrogel. It was proposed that since the protein shell of ferritin is encompassed by peptidic α-helical bundles, the ferritin and its chemical derivatives act as springs and allow for consistent nanocage and hydrogel interaction during

hydrogel compression and elongation, which could also explain the reinforcement of tensile stress and strain in hybrid hydrogels. More specifically, the mechanism behind the improvement of the mechanical properties in the hybrid hydrogel can be the result of the protein shell having a higher stiffness than that of the GelMA matrix, thus reducing tensile hoop stress at the hole boundary of the incorporated reinforcing material.[24] Because of the relationship of $E_{\text{iron core}} > E_{\text{protein shell}} > E_{\text{GelMA}}$ (E denotes elastic modulus), the elastic moduli of the hybrid hydrogels increased significantly. Overall, the interaction of the ferritin and its chemical derivatives with the GelMA matrix, plus the relationship of the elastic modulus, affects the toughness improvement of the hybrid hydrogels. Therefore, in our study, the nanocage concentration and UV exposure time, which could affect the distance between arranged particles and the bonding connection between particles and the GelMA matrix, are the most important factors in determining the mechanical reinforcement of hybrid hydrogels.

It was reported that the mechanical properties and the porosity of the scaffold matrix are acknowledged to influence cellular performance such as elongation, proliferation, and differentiation.[1,11,33] Hence, it is of great importance to maintain the biological advantage of the hydrogel (i.e., high cellular viability, proliferation, and spreading) while tuning the mechanical properties for various tissue engineering applications. To evaluate cellular behavior in the hybrid and nanocomposite hydrogels, NIH-3T3 fibroblasts were encapsulated in various concentrations of ferritin, FerMA, apoferritin, and ApoMA incorporated into 5 wt % GelMA hydrogels after 10 s UV exposure. As shown in Figure 4a, the difference in cell viability after 1 day of culture between pristine GelMA hydrogels and nanocage incorporated GelMA hydrogels was not significant. It was elucidated experimentally that the cell viability was higher than 95% for all samples (Figure 4b), proving the biocompatibility of the incorporated nanocages, even after methacrylation. Phase contrast images showed that cell spreading in encapsulated fibroblasts in 5 wt % GelMA incorporated with 0.1 and 1.0 mg/mL ferritin and FerMA could be observed as soon as on day 2, whereas in the case of pristine GelMA hydrogels (Figure S1), cell spreading did not show on day 2. The percentages of elongated fibroblasts in 5 wt % GelMA with different concentrations of ferritin and FerMA were quantified in Figure 4d for two different UV exposure times: 10 and 20 s. The results showed that cell spreading percentage in GelMA with ferritin/FerMA was higher than that in pristine GelMA hydrogels.

As a key indicator for cell spreading and cell motility, the filamentous actin of the cells inside the hybrid hydrogels after 7 days of culture was evaluated to display elongated, proliferated, and well-interconnected cellular shapes (Figure 4e,g). Here, for GelMA with ferritin, FerMA, and apoferritin, more actin filament networks were observed when compared with GelMA only. It was also shown that the cells were more elongated in the case of 0.1 than 1.0 mg/mL FerMA/ApoMA-GelMA hydrogels (Figure 4f,h). Consistent with our findings, several previous studies have also reported enhanced cell behavior, for example, higher cellular attachment and retention, when nanoparticles were incorporated in the hydrogels.[11,32,34] Such behavior could be explained by the increased surface roughness in the nanoscale, as roughness narrates the uppermost layer of a material’s texture. This can be attributed to the presence of nanomaterials (ferritin, FerMA, apoferritin, and ApoMA) within the GelMA hydrogel and can improve surface topographical cues for culturing

through integrin receptors.[35] Studies have shown that roughness is the most considered aspect of topography. Abundant experiments have stated that surface roughness can affect cell behaviors such as migration, proliferation, adhesion, and differentiation. Therefore, ferritin/apoferritin promoted cell viability and elongation without inducing cytotoxicity during the 7 days of culture, validating the feasibility of utilizing composite hydrogels with beneficial cellular microenvironments, and could have an important role in enhancing cell response and function for engineering tissue applications.

Recently, nanoparticles have become one of the most investigated methods for effective drug delivery. These nanocarriers are characterized by sustained release, targeted delivery, and dose control. Among many different nanoparticles that have been established for drug delivery such as polymeric liposomes, nanoparticles, and nanochitosan, apoferritin has emerged as an exceptional protein-based nanocage because of its surface properties, unique structure, and high biocompatibility. Considering these facts, in the present study, FITC-laden apoferritin/ApoMA-GelMA hydrogels were designed and assessed to show that the small compounds released characteristics of these composite hydrogels. Apoferritin can reversibly dissociate and associate in a shape memory fashion based on the surrounding pH. It has been proposed that while disassembled, apoferritin can be mixed with drug molecules, and drug molecules can be encapsulated within the apoferritin cavity once apoferritin is reassembled.[36,37] We investigated the drug release potential of apoferritin-GelMA by detecting the release profile of encapsulated FITC. As shown in Figure 5a, FITC was encapsulated in apoferritin as described in previous studies for the encapsulation of doxorubicin in apoferritin.[38]

To validate the nanocage function of apoferritin/ApoMA, the absorption spectra of plain FITC, filtered FITC mixed with apoferritin (FITC was not encapsulated), and filtered FITC captured in apoferritin and apoferritin solution were measured. The apoferritin showed high absorbance in the UV spectrum with a specific absorbance peak of aromatic amino acids at 280 nm (Figure 5b). Apoferritin mixed with FITC only showed absorbance peaks for apoferritin. Differently, FITC encapsulated apoferritin showed an absorbance spectrum containing both peaks characteristic for FITC and apoferritin, implying the successful encapsulation of FITC in the protein cage. Our results confirmed that there were few unspecific bonds between FITC and the apoferritin surface, which was further validated by fluorescent images (Figure 5c), providing evidence to the reliability of the FITC release method.

To evaluate the cumulative release profile, the release test was performed on apoferritin/ApoMA-GelMA hydrogels with encapsulated FITC at different time points under specific conditions. The results showed that ApoMA-GelMA and apoferritin-GelMA had drug storage potential at pH 7.4 and presented similar sustain-release profiles when the pH was at 2, revealing that UV initiated chain polymerization did not affect the drug delivery capability of the encapsulated nanocages (Figure 5d). Here, during the first 24 h, FITC was released at a constant rate and the release profile slope was constant. The release rate, however, gradually slowed down after 24 h. Eventually, almost 90% of the FITC had been released after 72 h in both ApoMA-GelMA and apoferritin-GelMA hydrogels cases. Features of apoferritin, like contributing to the use of apoferritin as a biological nanoparticle for

nanomedical applications, have been broadly studied. To take advantage of apoferritin nanocages, apoferritin/ApoMA conjugated GelMA hydrogels were designed and fabricated in our study for sustained drug delivery and tissue engineering applications. Our results showed that apoferritin/ApoMA-GelMA hydrogels maintained the structural integrity of the nanocages and obtained the drug delivery function of the nanocages: storage at pH 7.4 and release at pH 2. This nanocage incorporated hydrogel could be used to release a drug where the environment has an acidic pH. Taken together, apoferritin/ApoMA-GelMA hydrogels will be a promising candidate for drug-laden hybrid hydrogels for biomedical applications. Optimizing the hydrogel and nanoparticle properties could result in a longer period of controllable and sustained drug release, which is crucial for clinical transplants. Hence, further studies are needed to optimize the release profile of apoferritin/ApoMA-GelMA hydrogels.

CONCLUSIONS

In this study, we successfully developed biological nanocages such as ferritin and apoferritin and incorporated them with hybrid GelMA hydrogels with both physical and covalent bonding between the nanocages and the polymeric networks. The ferritin and apoferritin were successfully functionalized via the methacrylation process to create covalent bonding between the GelMA polymeric chains and the protein shells of the nanocages with the photo-cross-linking method. Incorporation of ferritin-based nanocages with GelMA hydrogels successfully tuned and improved the mechanical properties of the hydrogels. Especially, covalently bonded FerMA-GelMA and ApoMA-GelMA hydrogels showed higher elastic moduli and better tunability of mechanical properties due to increased cross-linking densities. At the same time, the hybrid hydrogels showed excellent cell behaviors along with high viability, spreading, and elongation of encapsulated cells. Moreover, the drug release function of apoferritin/ApoMA incorporated GelMA hydrogels was assessed over 70 h with an FITC cumulative release profile under specific pH conditions. These results thus confirm that nanocages conjugated with hybrid hydrogels can be used as nanocarriers for sustained and controlled drug release under specific conditions along with improved mechanical properties for tissue engineering applications.

Supplementary Material

Refer to Web version on PubMed Central for supplementary material.

ACKNOWLEDGMENTS

This paper was funded by the National Institutes of Health (R01AR074234, R21EB026824, R01 AR073822-01), the Brigham Research Institute Stepping Strong Innovator Award, AHA Innovative Project Award (19IPLOI34660079), and the Qatar national Research Fund (a part of Qatar Foundation, NPRP9-144-3-021).

REFERENCES

(1). Lee D; Heo DN; Nah HR; Lee SJ; Ko WK; Lee JS; Moon HJ; Bang JB; Hwang YS; Reis RL; Kwon IK Injectable hydrogel composite containing modified gold nanoparticles: implication in bone tissue regeneration. Int. J. Nanomed 2018, 13, 7019–7031.

(2). Nawroth JC; Scudder LL; Halvorson RT; Tresback J; Ferrier JP; Sheehy SP; Cho A; Kannan S; Sunyovszki I; Goss JA; Campbell PH; Parker KK Automated fabrication of photopatterned gelatin hydrogels for organ-on-chips applications. Biofabrication 2018, 10, No. 025004.

(3). Li L; Pan L; Ma Z; Yan K; Cheng W; Shi Y; Yu G All Inkjet-Printed Amperometric Multiplexed Biosensors Based on Nanostructured Conductive Hydrogel Electrodes. Nano Lett 2018, 18, 3322–3327. [PubMed: 29419302]

(4). Kiene K; Porta F; Topacogullari B; Detampel P; Huwyler J Self-assembling chitosan hydrogel: A drug-delivery device enabling the sustained release of proteins. J. Appl. Polym. Sci 2018, 135, 45638.

(5). Kirschner CM; Anseth KS Hydrogels in Healthcare: From Static to Dynamic Material Microenvironments. Acta Mater 2013, 61, 931–944. [PubMed: 23929381]

(6). Hoare TR; Kohane DS Hydrogels in drug delivery: Progress and challenges. Polymer 2008, 49, 1993–2007.

(7). Vedadghavami A; Minooei F; Mohammadi MH; Khetani S; Rezaei A; Mashayekhan S; Nezhad A Manufacturing of hydrogel biomaterials with controlled mechanical properties for tissue engineering applications. Acta Biomater 2017, 62, 42–63. [PubMed: 28736220]

(8). Sun M; Sun X; Wang Z; Guo S; Yu G; Yang H Synthesis and Properties of Gelatin Methacryloyl (GelMA) Hydrogels and Their Recent Applications in Load-Bearing Tissue. Polymers 2018, 10, No. 1290.

(9). Yue K; Trujillo-de Santiago G; Alvarez MM; Tamayol A; Annabi N; Khademhosseini A Synthesis, properties, and biomedical applications of gelatin methacryloyl (GelMA) hydrogels. Biomaterials 2015, 73, 254–71. [PubMed: 26414409]

(10). Wu J; Tao K; Guo Y; Li Z; Wang X; Luo Z; Feng S; Du C; Chen D; Miao J; Norford LKA 3D Chemically Modified Graphene Hydrogel for Fast, Highly Sensitive, and Selective Gas Sensor. Adv. Sci 2017, 4, No. 1600319.

(11). Shin SR; Bae H; Cha JM; Mun JY; Chen Y-C; Tekin H; Shin H; Farshchi S; Dokmeci MR; Tang S; Khademhosseini A Carbon Nanotube Reinforced Hybrid Microgels as Scaffold Materials for Cell Encapsulation. ACS Nano 2012, 6, 362–372. [PubMed: 22117858]

(12). Wahid F; Zhong C; Wang H-S; Hu X-H; Chu L-Q Recent Advances in Antimicrobial Hydrogels Containing Metal Ions and Metals/Metal Oxide Nanoparticles. Polymers 2017, 9, 636.

(13). Biondi M; Borzacchiello A; Mayol L; Ambrosio L Nanoparticle-Integrated Hydrogels as Multifunctional Composite Materials for Biomedical Applications. Gels 2015, 1, 162–178. [PubMed: 30674171]

(14). Thakur S; Pandey S; Arotiba OA Development of a sodium alginate-based organic/inorganic superabsorbent composite hydrogel for adsorption of methylene blue. Carbohydr. Polym 2016, 153, 34–46. [PubMed: 27561469]

(15). Vorselen D; MacKintosh FC; Roos WH; Wuite GJL Competition between Bending and Internal Pressure Governs the Mechanics of Fluid Nanovesicles. ACS Nano 2017, 11, 2628–2636. [PubMed: 28273422]

(16). Schreier H; Bouwstra J Liposomes and niosomes as topical drug carriers: dermal and transdermal drug delivery. J. Controlled Release 1994, 30, 1–15.

(17). Zhao F; Yao D; Guo R; Deng L; Dong A; Zhang J Composites of Polymer Hydrogels and Nanoparticulate Systems for Biomedical and Pharmaceutical Applications. Nanomaterials 2015, 5, 2054–2130. [PubMed: 28347111]

(18). Theil EC Ferritin: structure, gene regulation, and cellular function in animals, plants, and microorganisms. Annu. Rev. Biochem 1987, 56, 289–315. [PubMed: 3304136]

(19). Theil EC Ferritin protein nanocages the story. Nanotechnol. Perceptions 2012, 8, 7–16.

(20). Truffi M; Fiandra L; Sorrentino L; Monieri M; Corsi F; Mazzucchelli S Ferritin nanocages: A biological platform for drug delivery, imaging and theranostics in cancer. Pharmacol. Res 2016, 107, 57–65. [PubMed: 26968122]

(21). Li L; Muñoz-Culla M; Carmona U; Lopez MP; Yang F; Trigueros C; Otaegui D; Zhang L; Knez M Ferritin-mediated siRNA delivery and gene silencing in human tumor and primary cells. Biomaterials 2016, 98, 143–151. [PubMed: 27187278]

(22). Todd TJ; Zhen Z; Xie J Ferritin nanocages: great potential as clinically translatable drug delivery vehicles? Nanomedicine 2013, 8, 1555–1557. [PubMed: 24074382]

(23). Monti DM; Ferraro G; Merlino A Ferritin-based anticancer metallodrug delivery: Crystallographic, analytical and cytotoxicity studies. Nanomedicine 2019, 20, No. 101997. [PubMed: 30472323]

(24). Shin MK; Kim SI; Kim SJ; Kim BJ; So I; Kozlov ME; Oh J; Baughman RH A tough nanofiber hydrogel incorporating ferritin. Appl. Phys. Lett 2008, 93, No. 163902.

(25). Shin MK; Spinks GM; Shin SR; Kim SI; Kim SJ Nanocomposite Hydrogel with High Toughness for Bioactuators. Adv. Mater 2009, 21, 1712–1715.

(26). Occhetta P; Sadr N; Piraino F; Redaelli A; Moretti M; Rasponi M Fabrication of 3D cell-laden hydrogel microstructures through photo-mold patterning. Biofabrication 2013, 5, No. 035002.

(27). May ME; Fish WW The uv and visible spectral properties of ferritin. Arch. Biochem. Biophys 1978, 190, 720–725. [PubMed: 568914]

(28). Hutson CB; Nichol JW; Aubin H; Bae H; Yamanlar S; Al-Haque S; Koshy ST; Khademhosseini A Synthesis and characterization of tunable poly(ethylene glycol): gelatin methacrylate composite hydrogels. Tissue Eng., Part A 2011, 17, 1713–23. [PubMed: 21306293]

(29). Shanmuganathan K; Capadona JR; Rowan SJ; Weder C Stimuli-responsive mechanically adaptive polymer nanocomposites. ACS Appl. Mater. Interfaces 2010, 2, 165–74. [PubMed: 20305827]

(30). Bhattacharyya S; Sinturel C; Salvetat JP; Saboungi M-L Protein-functionalized carbon nanotube-polymer composites. Appl. Phys. Lett 2005, 86, No. 113104.

(31). Morel I; Cillard J; Lescoat G; Sergent O; Pasdeloup N; Ocaktan AZ; Abdallah MA; Brissot P; Cillard P Antioxidant and free radical scavenging activities of the iron chelators pyoverdin and hydroxypyrid-4-ones in iron-loaded hepatocyte cultures: comparison of their mechanism of protection with that of desferrioxamine. Free Radical Biol. Med 1992, 13, 499–508. [PubMed: 1334028]

(32). Shin SR; Jung SM; Zalabany M; Kim K; Zorlutuna P; Kim Sb; Nikkhah M; Khabiry M; Azize M; Kong J; Wan K.-t.; Palacios T; Dokmeci MR; Bae H; Tang X; Khademhosseini A Carbon-Nanotube-Embedded Hydrogel Sheets for Engineering Cardiac Constructs and Bioactuators. ACS Nano 2013, 7, 2369–2380. [PubMed: 23363247]

(33). Shin SR; Aghaei-Ghareh-Bolagh B; Dang TT; Topkaya SN; Gao X; Yang SY; Jung SM; Oh JH; Dokmeci MR; Tang XS; Khademhosseini A Cell-laden microengineered and mechanically tunable hybrid hydrogels of gelatin and graphene oxide. Adv. Mater 2013, 25, 6385–91. [PubMed: 23996513]

(34). Liu Y; Meng H; Konst S; Sarmiento R; Rajachar R; Lee BP Injectable Dopamine-Modified Poly(ethylene glycol) Nanocomposite Hydrogel with Enhanced Adhesive Property and Bioactivity. ACS Appl. Mater. Interfaces 2014, 6, 16982–16992. [PubMed: 25222290]

(35). Metavarayuth K; Sitasuwan P; Zhao X; Lin Y; Wang Q Influence of Surface Topographical Cues on the Differentiation of Mesenchymal Stem Cells in Vitro. ACS Biomater. Sci. Eng 2016, 2, 142–151.

(36). Kim M; Rho Y; Jin KS; Ahn B; Jung S; Kim H; Ree M pH-dependent structures of ferritin and apoferritin in solution: disassembly and reassembly. Biomacromolecules 2011, 12, 1629–40. [PubMed: 21446722]

(37). Yang Z; Wang X; Diao H; Zhang J; Li H; Sun H; Guo Z Encapsulation of platinum anticancer drugs by apoferritin. Chem. Commun 2007, 3453–3455.

(38). Kilic MA; Ozlu E; Calis S A Novel Protein-Based Anticancer Drug Encapsulating Nanosphere: Apoferritin-Doxorubicin Complex. J. Biomed. Nanotechnol 2012, 8, 508–514. [PubMed: 22764421]

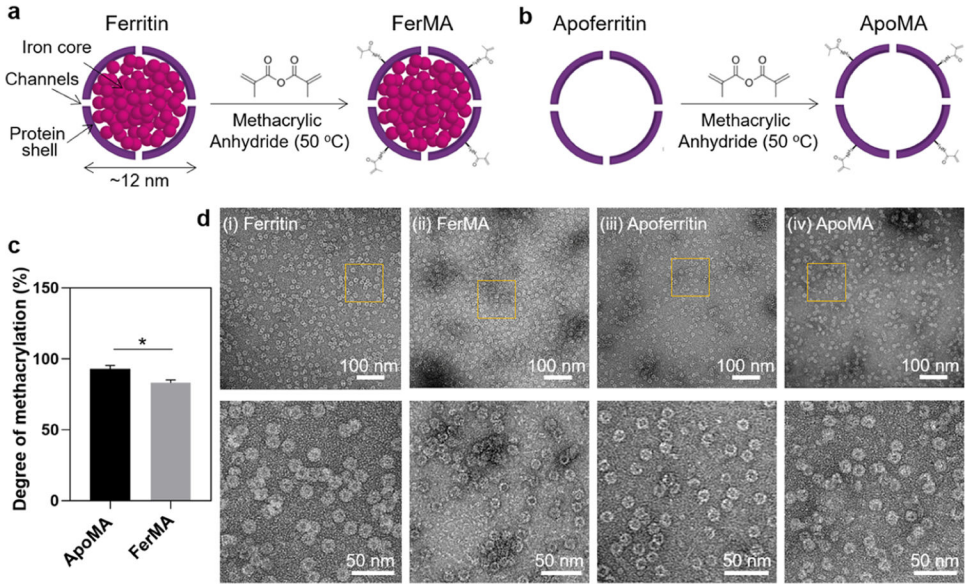

Figure 1.

Schematic of (a) ferritin and (b) apoferritin methacrylation process. (c) Methacrylation degrees of FerMA and ApoMA ($n = 3$). (d) TEM images of (i) ferritin, (ii) FerMA, (iii) apoferritin, and (iv) ApoMA-laden solutions. (*$p < 0.05$).

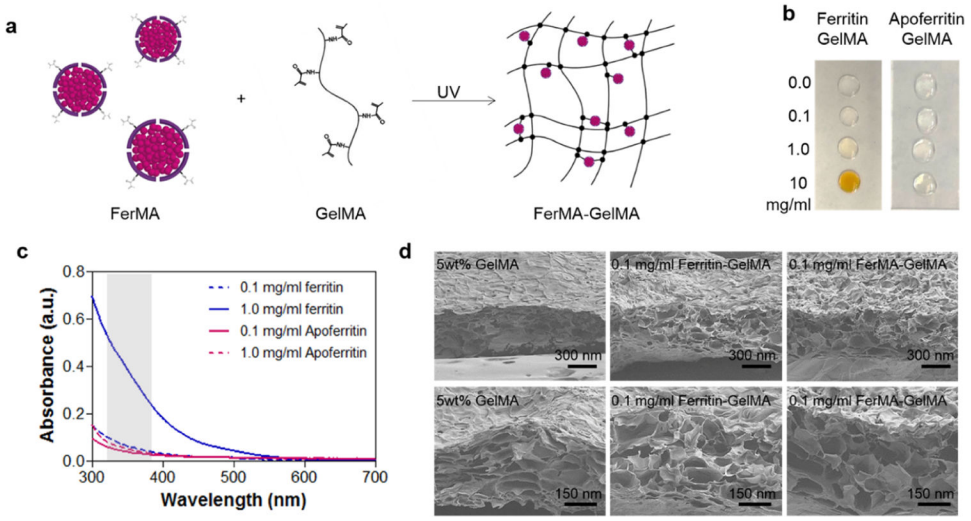

Figure 2.

(a) Fabrication process of FerMA-GelMA hydrogels with covalent conjugation via the photo-cross-linking method. (b) Optical images of ferritin-GelMA and apoferritin-GelMA prepolymer solutions with different concentrations of nanoparticles. (c) UV–vis absorbance spectra of ferritin-GelMA and apoferritin-GelMA prepolymer solutions with different concentrations of nanoparticles. Gray range from 320 to 390 nm indicates the wavelength of UV light. (d) SEM images of cross section of ferritin-GelMA and FerMA-GelMA hydrogels with 0.1 mg/mL nanoparticles.

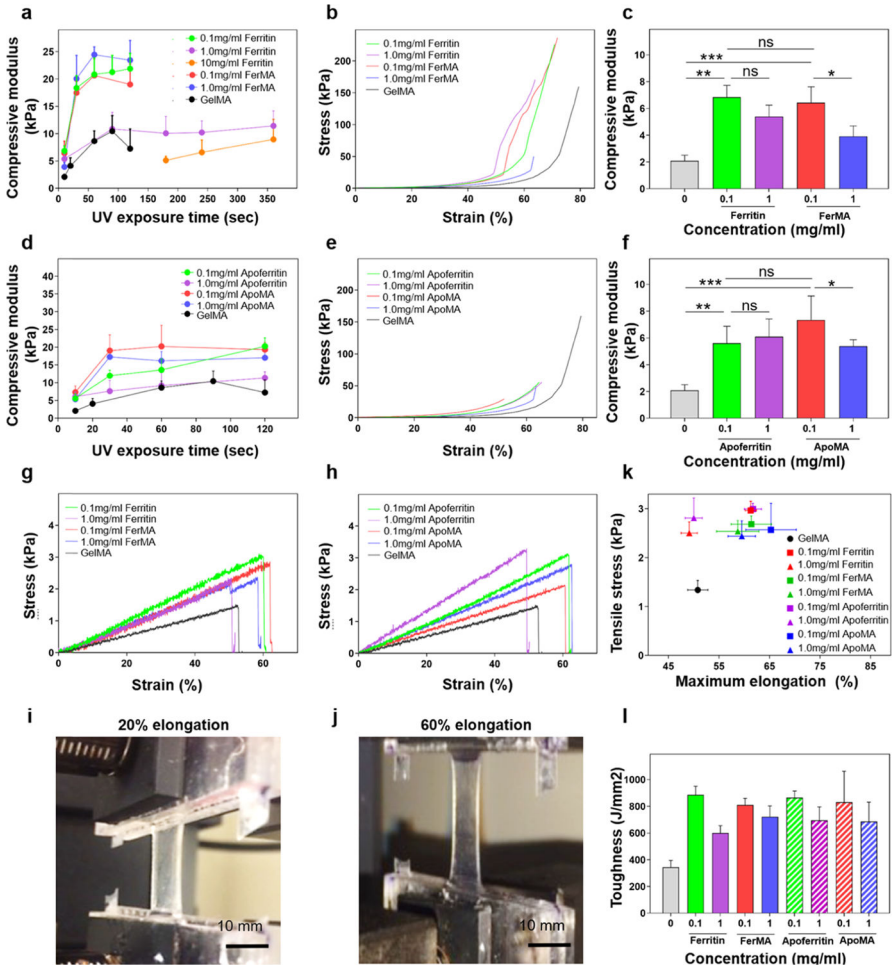

Figure 3.

(a) Compressive modulus of ferritin-GelMA and FerMA-GelMA hydrogels with different concentrations of nanoparticles and UV exposure times ($n = 5$). (b) Representative stress–strain curves for the compression test and (c) compressive modulus of ferritin-GelMA and FerMA-GelMA hydrogels with different concentrations of nanoparticles (UV exposure time: 10 s) ($n = 5$). (d) Compressive modulus of apoferritin-GelMA and ApoMA-GelMA hydrogels with different concentrations of nanoparticles and UV exposure times ($n = 5$). (e) Representative stress–strain curves for the compression test and (f) compressive modulus of apoferritin-GelMA and ApoMA-GelMA hydrogels with different concentrations of nanoparticles (UV exposure time: 10 s) ($n = 5$). Stress–strain curves for tensile tests of (g) ferritin-GelMA and FerMA-GelMA hydrogels and (h) apoferritin-GelMA and ApoMA-GelMA hydrogels with different concentrations of nanoparticles. (i, j) Images of ferritin-GelMA at 20 and 60% elongation under tensile tests. (k) Calculated toughness and (l) tensile stress vs maximum elongation of ferritin-GelMA, FerMA-GelMA hydrogels, apoferritin-GelMA, and ApoMA-GelMA hydrogels with varying concentrations of nanoparticles ($n = 5$). (*$p < 0.05$, **$p < 0.01$, ***$p < 0.001$).

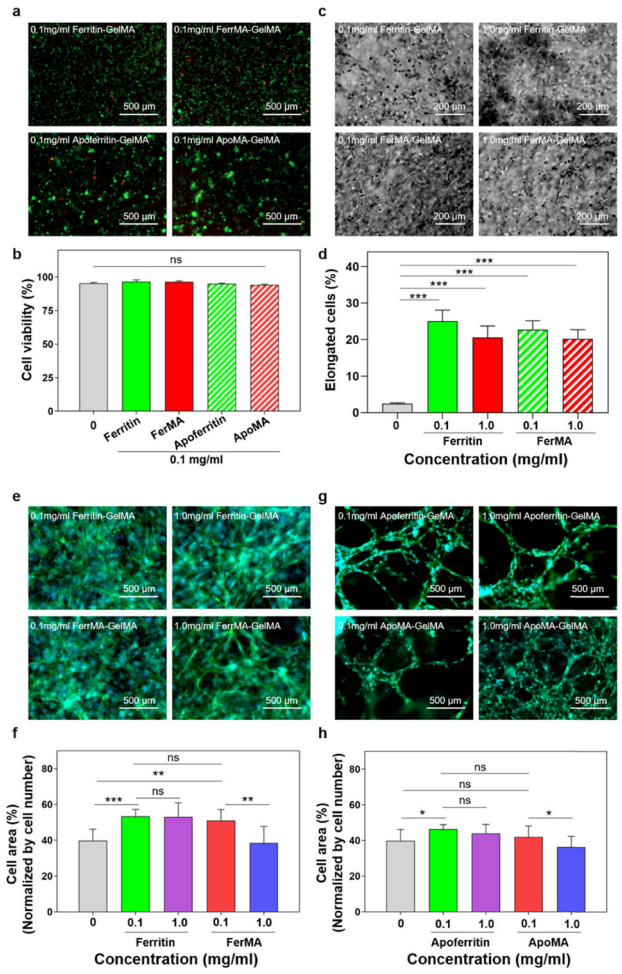

Figure 4.

(a) Representative live/dead images of NIH-3T3 fibroblasts embedded in hydrogels and (b) quantification of cell viability demonstrating excellent cell survival for all conditions after 24 h of encapsulation ($n = 3$). (c) Representative phase contrast images and (d) quantification of elongated NIH-3T3 fibroblasts encapsulated in ferritin-GelMA and FerMA-GelMA hydrogels for 10 s UV exposure time after day 2 in culture. (e, g) F-actin/DAPI staining images and (f, h) percentages of cell area of NIH-3T3 fibroblast encapsulated in FerMA-GelMA and ApoMA-GelMA hydrogels with 1.0 mg/mL nanoparticles after 7 days of culture (UV exposure time: 10 s) ($n = 3$). DAPI (blue) for nuclei, phalladoin (green) for F-actin. (*$p < 0.05$, **$p < 0.01$, ***$p < 0.001$).

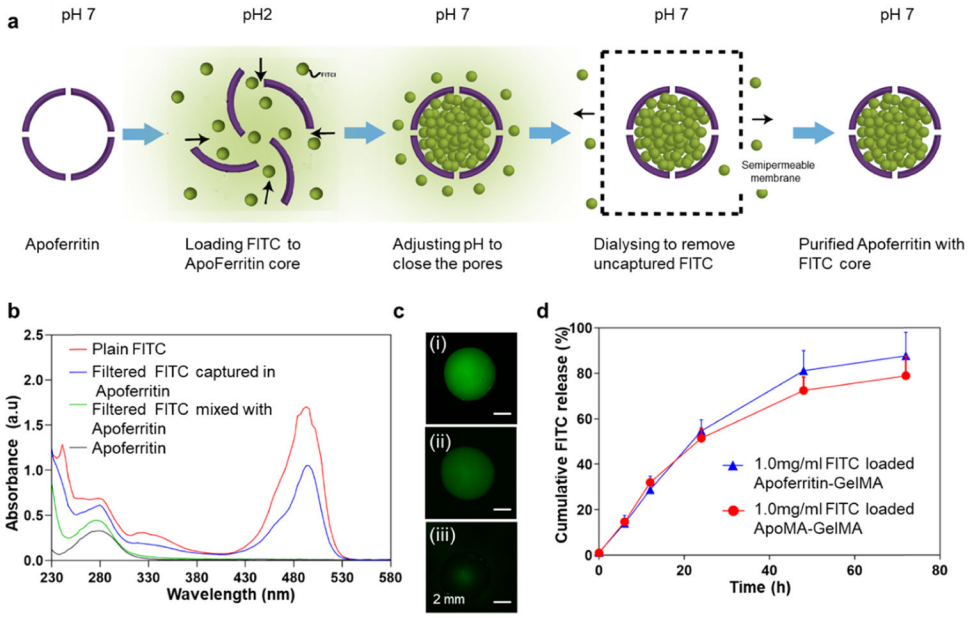

Figure 5.

(a) Schematic of encapsulation of FITC within apoferritin. (b) UV–vis absorption spectra of pristine FITC (red color), FITC-laden apoferritin (blue color), FITC mixed with apoferritin (green color), and apoferritin (black color) solutions. (c) Florescence images of (i) pristine FITC, (ii) FITC-laden apoferritin, and (iii) FITC mixed with apoferritin. (d) FITC release profile of FITC-laden apoferritin-GelMA and FITC-laden ApoMA-GelMA hydrogels under pH change (pH 2) ($n = 2$).